A Dual-Reporter System for Real-Time Monitoring and High-throughput CRISPR/Cas9 Library Screening of the Hepatitis C Virus

Qingpeng Ren[1]*, Chan Li[1]*, Pengfei Yuan[1], Changzu Cai[1], Linqi Zhang[2], Guangxiang George Luo[3,4] & Wensheng Wei[1]

[1]Biodynamic Optical Imaging Center (BIOPIC), Peking-Tsinghua Center for Life Sciences, State Key Laboratory of Protein and Plant Gene Research, School of Life Sciences, Peking University, Beijing 100871, China, [2]Comprehensive AIDS Research Center and Research Center for Public Health, School of Medicine, Tsinghua University, Beijing 100084, China, [3]Department of Microbiology, University of Alabama at Birmingham School of Medicine, Birmingham, Alabama 35294, USA, [4]Department of Microbiology, Peking University College of Basic Medical Sciences, Beijing 100083, China.

The hepatitis C virus (HCV) is one of the leading causes of chronic hepatitis, liver cirrhosis and hepatocellular carcinomas and infects approximately 170 million people worldwide. Although several reporter systems have been developed, many shortcomings limit their use in the assessment of HCV infections. Here, we report a real-time live-cell reporter, termed the NIrD (NS3-4A Inducible rtTA-mediated Dual-reporter) system, which provides an on-off switch specifically in response to an HCV infection. Using the NIrD system and a focused CRISPR/Cas9 library, we identified *CLDN1*, *OCLN* and *CD81* as essential genes for both the cell-free entry and the cell-to-cell transmission of HCV. The combination of this ultra-sensitive reporter system and the CRISPR knockout screening provides a powerful and high-throughput strategy for the identification of critical host components for HCV infections.

Since it was first identified in 1989[1], HCV has become increasingly important in diseases associated with viral hepatitis, as well as HIV infections[2,3]. Although progress has been made in identifying key events that occur in host cells upon HCV infection over the past two decades[4–9], the lack of a highly effective method to monitor the viral infection has hindered advances in the study of HCV. Specifically, it is difficult to distinguish between the two routes of HCV infection, cell-free entry and cell-to-cell transmission[10–14]. We aim to create a system that overcomes the various imperfections of the current methods of HCV monitoring[15–22] and, conse-quently, to establish a high-throughput strategy to globally investigate the role of host genes in HCV infections.

The design of this novel HCV reporter consists of two modules, a sensor and an amplifier. The sensor is the chimeric protein rtTA-MAVS(C) (reverse tetracycline transactivator[23,24] - mitochondrial antiviral signalling protein[25] (C-terminal amino acids 462–540)) that contains the NS3-4A cleavage site. The amplifier is an express-ion module composed of the tight-TRE promoter[26] followed by the coding sequences of 2A-linked delta-TK[27] and mCherry (Fig. 1a). To minimise a potential leakage problem, the sensor and amplifier are spatially separated, with the former anchored to the cytoplasmic mitochondria and the latter located in the nucleus. In addition, the activation of the tight-TRE promoter requires both rtTA and doxycycline (Dox)/tetracycline, further minimising its non-specific activation. This live cell reporter, designated as the NIrD (NS3-4A Inducible rtTA-mediated Dual-reporter) system, provides an on-off switch that specifically responds to an HCV invasion. Upon inocu-lation, HCV-encoded NS3-4A protease cleaves rtTA-MAVS(C) in mitochondria, and the free-formed rtTA subsequently enters the nucleus, where it binds to and activates the tight-TRE promoter in the presence of Dox, resulting in de novo expression of delta-TK-2A-mCherry. After 2A-mediated cleavage, mCherry gives rise to red fluorescence and delta-TK leads to cell death in the presence of GCV (Ganciclovir)[27] (Fig. 1a). All elements of the sensor and amplifier were combined into a single lentiviral backbone, pLenti-NIrD (Supplementary Fig. 1), making it convenient to acquire stable clones with the integrated NIrD system in any given cell type through viral infection and Blasticidin selection.

To examine the efficiency and specificity of this new reporter, we first established the NIrD system in a non-hepatic cell line, HeLa. Strong red fluorescence was observed in HeLa(NIrD) cells only when they were infected by Lenti(NS3-4A) and supplied with Dox (2 μg/ml). Interestingly, HCVcc (JFH-1 strain)[28], unlike lentivirally expressed NS3-4A, failed to induce red fluorescence even in the presence of Dox, which is consistent with previous reports that non-hepatic cells lack key receptors that allow HCV entry[29] (Supplementary Fig. 2a). Similarly, only the lentivirally expressed NS3-4A, not HCVcc, induced delta-TK-mediated death in the presence of GCV in HeLa cells (Supplementary Fig. 2b). The finding that Dox is required for all reporter gene expression demonstrates that reporter production is under the complete control of the tight-TRE promoter (Supplementary Fig. 2).

We then introduced the NIrD system to a hepatic cell line, Huh7.5, and selected Blasticidin-resistant clones for further analysis. Lentivirally delivered NS3-4A in the presence of Dox again induced red fluorescence (Supplementary Fig. 3a) and delta-TK-mediated death in the presence of GCV at 96 h post-infection (Supplementary Fig. 4). The red fluorescence peaked 72–96 h following the viral infection (Supplementary Fig. 3b). HCVcc inoculation induced mCherry fluorescence only in the presence of Dox, indicating that the NIrD system is capable of specifically detecting an HCV infection (Fig. 1b). The production of the 2nd reporter delta-TK upon HCV infection (+Dox) led to cell death when GCV was supplied (Fig. 1c). These dual reporters, both responding specifically to an HCV challenge, provide additional flexibility for the use of this system.

We further confirmed that the mCherry fluorescence was tightly associated with HCV infection, where HCV viral particles were detected by anti-core antibody plus Alexa Fluor 488-conjugated secondary antibody (Fig. 1d). Consistently, red and green fluorescence coexisted when Huh7.5(NIrD) cells were infected by HCVcc encoding NS5A-EGFP[28] (Supplementary Fig. 5). Immunoblotting analysis confirmed that Dox did not affect the viral infection as determined by the similar level of HCV core protein inside the cells (Fig. 1e). Based on our design, the transactivation of the dual reporters is mediated by NS3-4A activity, which cleaves and releases rtTA from the mitochondria (Fig. 1a). Indeed, the red fluorescent signals correlated inversely with the amount of VX-950 (i.e., Telaprevir), an NS3-4A inhibitor and newly marketed drug approved by FDA[30]. The finding that 500 nM of VX-950 blocked nearly all of the mCherry production indicates that the NIrD system is suitable for the screening of chemical compound inhibitors against HCV (Fig. 1f).

To quantitatively evaluate the NIrD system in response to HCV infections, we monitored the mCherry signal upon viral inoculation at different time points. The red fluorescence did not appear until 48 h after the infection, and the number of cells showing fluorescence increased over time (Fig. 2a). Uninfected cells showed no detectable signals in FACS analysis, while Huh7.5(NIrD) responded with high sensitivity to the viral infection; in total, 96.6% of infected Huh7.5(NIrD) cells displayed red fluorescence when the titre of HCVcc reached 2.51×10^4 TCID50/ml (Fig. 2b). These results indicate a superior signal/noise ratio, a finding that was further confirmed by detailed FACS analysis, which showed that the reporter signals and HCV titres had a strong linear correlation ($R^2 = 0.995$) within a dynamic range (Fig. 2c-d). In particular, the NIrD system was sensitive enough to detect HCV with a MOI as low as 0.001 (Fig. 2d).

Next, we investigated whether the NIrD system could be used for large-scale screening purposes. Taking advantage of a functional screening technique that we have recently developed[31], we screened a focused CRISPR library in Huh7.5(NIrD) cells, in which OCT1-Cas9 expression was pre-established through lentiviral infection and neomycin selection (Fig. 3a). One particular clone, designated as Huh7.5(NIrd)$_{OC}$-SC14, was selected to construct the library because it showed the highest level of efficiency in creating indels using CSPG4-targeting sgRNA[31] and increased its efficiency in causing DNA double-strand breaks (DSBs) with prolonged culturing, as expected (Fig. 3b).

We used the same library as previously reported[31], supplemented with additional sgRNAs, for a total of 918 sgRNAs that targeted 296 human genes, including all of the genes[14] that have been reported to encode cell surface proteins important for HCV infections (Supplementary Table 1). Fifteen non-targeting sequences were also included in the library as negative controls. The CRISPR library built on Huh7.5(NIrD)$_{OC}$-SC14 underwent 3–4 rounds of HCV challenges and FACS enrichment for those cells that no longer showed red fluorescence following the HCV inoculation (Fig. 3c). At the end of the last round of the HCV infection, over 99.4% of the cells in all three replications of the libraries showed no mCherry signal, while the majority of the control Huh7.5(NIrD)$_{OC}$ cells remained responsive to HCV (Supplementary Fig. 6a). All Huh7.5(NIrD)$_{OC}$ cells remained responsive to lentivirally delivered NS3-4A (Supplementary Fig. 6b), indicating that the NIrD system was functional even in the enriched Huh7.5(NIrD)$_{OC}$ cells post-screening.

High-throughput sequencing analysis revealed a total of 912 sgRNA sequences (99.3% of the 918 designed) from the original library (Supplementary Table 2). We compared the abundance of each sgRNA between the final enriched Huh7.5(NIrD)$_{OC}$ cells that no longer responded to HCV inoculation and the untreated populations and calculated a score for each sgRNA or gene using different algorithms (Fig. 4a–c). Three genes, CLDN1, OCLN and CD81, were confirmed to encode receptor proteins essential for HCV infections, based on false discovery rate (FDR) calculations[32]. It remains to be determined whether the other genes in the library are minimally involved in HCV infections or whether the number of designed sgRNAs targeting these genes were simply too small to produce data with statistical significance.

To further verify if these three proteins play an indispensible role in HCV infections as previously reported[4,6,7], we created individual CLDN1, OCLN and CD81 knockouts in Huh7.5(NIrD) cells using either the TALEN technique[33] or the CRISPR/Cas9 system[31]. Clones in Huh7.5(NIrD) cells with the complete knockout of these genes were isolated, and Sanger sequencing analysis revealed that Huh7.5 (NIrD) $CLDN1^{-/-}$ contained a 31-nt insertion in the TALEN-targeting region, Huh7.5(NIrD) $OCLN^{-/-}$ contained a 17-nt insertion in the CRISPR sgRNA-targeting region, and Huh7.5(NIrD) $CD81^{-/-}$ contained a 8-nt deletion in the CRISPR sgRNA-targeting region; all of these changes led to frame shifts (Supplementary Fig. 7a–c). The loss of the gene expression of any of these three genes completely blocked HCV infections, while the exogenous expression of their corresponding genes in the knockout lines rescued these lost phenotypes (Fig. 4d). These results are consistent with prior reports for the essential roles of CD81, CLDN1 and OCLN as receptors or co-receptors facilitating the HCV internalisation process[4,6,7].

We next investigated role of these genes in the cell-to-cell transmission of HCV, another important route for the spread of the virus[34,35]. Huh7.5(NIrD) cells were mixed with donor Huh7.5 cells pre-loaded with EGFP-labelled HCVcc[28], and red fluorescence appeared after 72 h (+Dox), indicating that HCV was transmitted through tight junctions to Huh7.5(NIrD) cells. Interestingly, this cell-to-cell transmission route was blocked in all three gene-knockout clones, while the expression of their corresponding genes restored the lost phenotypes (Fig. 4e). These results are consistent with previous findings that CLDN1 and OCLN are tight junction proteins critical for the cell-to-cell transmission of HCV[11,34]. The role of CD81 in the spread of the virus between cells is somewhat controversial[10–12], and our results support its active role in HCV transmission between neighbouring cells.

Current HCV reporter systems are either viral-based or host cell-based. The viral-based strategy uses modified HCVcc or replicons of different subtypes to express reporters such as EGFP[36,37] or lucifer-
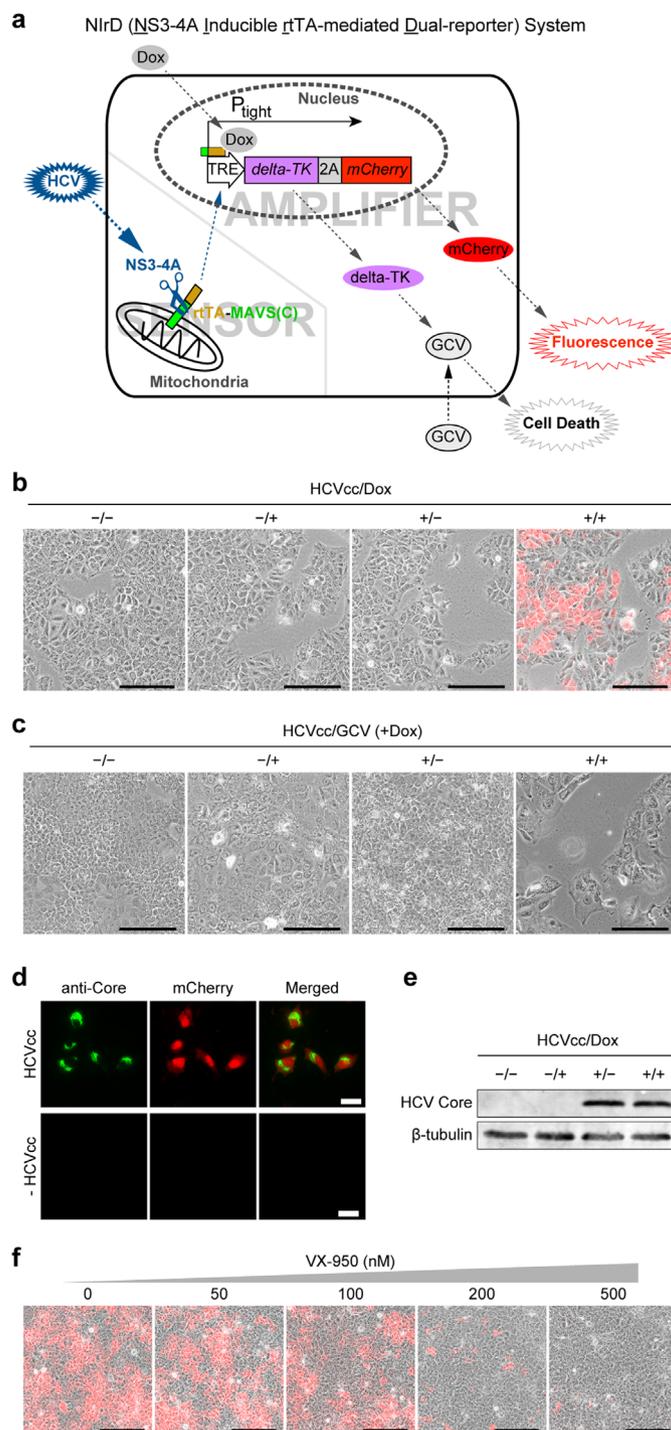
Figure 1 | A cell-based dual-reporter system for monitoring HCV infections. (a) The rationale of the NIrD system. The sensor module consists of rtTA-MAVS(C) fusion proteins, which are constantly produced and localised to the mitochondria in cells. The amplifier module is an expression cartridge integrated into the chromosome that is composed of two reporter genes driven by the tight-TRE promoter. Upon HCV infection, the virally produced NS3-4A cleaves its recognition sequence in MAVS(C), releasing the free-formed rtTA into the nucleus. The tight-TRE promoter is activated by rtTA and Dox (2 μg/ml), resulting in the production of delta-TK-2A-mCherry proteins. After self-cleavage of the 2A peptide, mCherry shows red fluorescence and delta-TK phosphorylates GCV (2 μg/ml) to cause cell death. (b) mCherry signal of the NIrD system in response to an HCVcc infection. The Huh7.5(NIrD) system was infected by HCVcc for 72 h. HCVcc-transduced (+) or -untransduced (−) cells in the presence (+) or absence (−) of Dox (2 μg/ml) were visualised under a microscope. The fluorescence signals were superimposed onto white light images. Scale bar, 200 μm. (c) The death signal of the NIrD system in response to an HCVcc infection in the presence of GCV (2 μg/ml). Huh7.5(NIrD) cells were infected with HCVcc for 120 h. The transduced (+) or untransduced (−) cells in the presence (+) or absence (−) of Dox (2 μg/ml) were visualised under a light microscope. Scale bar, 200 μm. (d) Fluorescence microscopy of HCVcc core protein (Alexa Fluor 488) and mCherry signal upon HCVcc infection (72 h) in Huh7.5(NIrD) cells. Scale bar, 30 μm. (e) Immunoblotting analysis of Huh7.5(NIrD) cells infected with or without HCVcc in the presence or absence of Dox (2 μg/ml). HCVcc was detected by an antibody specifically targeting the viral core protein, and β-tubulin was used as the loading control. (f) Dosage effects of VX-950 on the live-cell imaging of HCVcc-infected Huh7.5(NIrD) cells. Huh7.5(NIrD) cells were infected with HCVcc plus Dox (2 μg/ml) together with serially increasing dosages of VX-950 (Telaprevir). Fluorescence microscopic images were taken 72 h following the HCVcc infection. Scale bar, 200 μm.
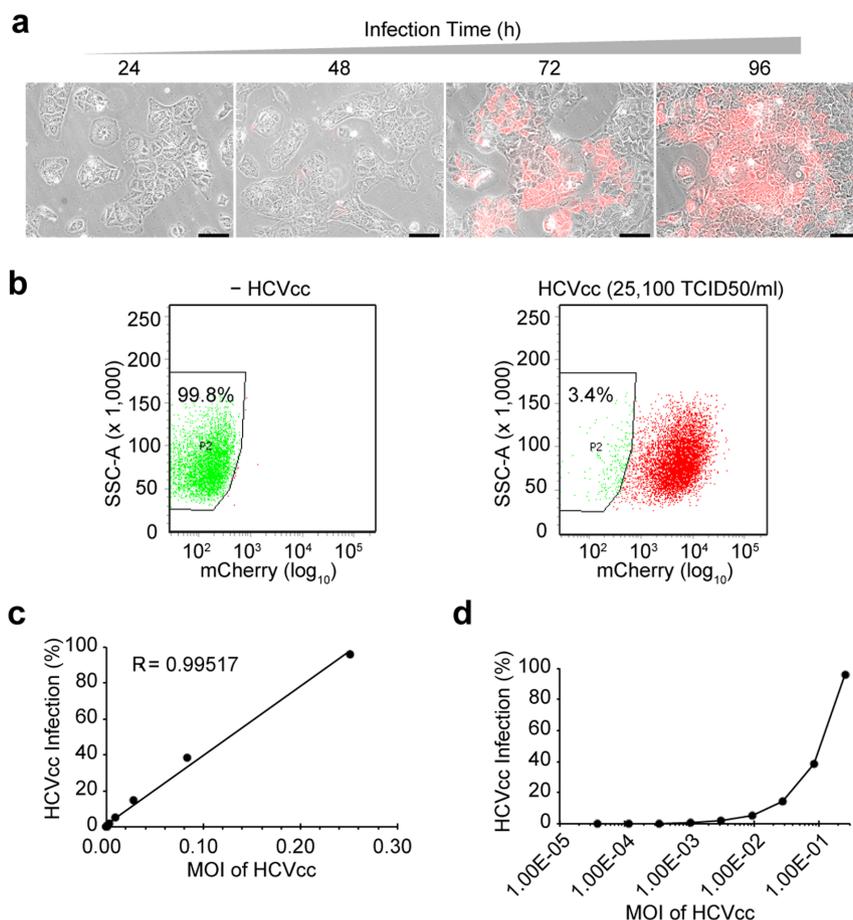
Figure 2 | Quantitative evaluation of NIrD system in response to HCV inoculation. (a) Time-lapse live-cell imaging of Huh7.5(NIrD) cells. Both light and fluorescence images were taken every 24 h, starting at 24 h post-HCVcc infection in the presence of Dox (2 μg/ml). Scale bar, 100 μm. (b) FACS analysis of Huh7.5(NIrD) cells infected by HCVcc in the presence of Dox (2 μg/ml). A total of 2×10^5/well of Huh7.5(NIrD) cells were seeded in 6-well plates. Representative results from reporter cells treated with HCVcc (0 or 25,100 TCID50/ml) are presented. FACS analysis was conducted 96 h following the viral infection. The numbers in the square indicate the percentage of red fluorescence-negative cells. (c-d) FACS analysis of Huh7.5(NIrD) cells infected by serially increasing dosages of HCVcc. The curves show the percentage of mCherry positive cells corresponding to MOI (2×10^5 cells/well) in linear (c) or logarithmic (d) plots.

ase[38]. However, the modification of HCV genome may be cumbersome, as the productivity of an artificial HCV may drop over time and the modified genome may create additional RNA structure deviations[37]. In addition, viral-based reporters are unable to distinguish between cell-free entry and cell-to-cell transmission routes for HCV. In comparison, cell-based reporter systems take advantage of the bio-activity of HCV-encoded proteins, such as NS3-4A protease[18,39–42] and NS5B RNA polymerase[43]. The NIrD system we report here uses multiple layers of regulations, including a sensor and an amplifier, to ensure minimal background noise and maximal signals through amplification specifically in response to HCV inoculation. The NIrD system is particularly advantageous in the study of HCV transmission, as it does not require complex processes such as antibody staining[8]. The applicability of the NIrD system to a broad range of HCV genotypes is also supported by the finding that the NS3-4A cutting site is sensitive to numerous HCV genotypes[18,44]. Nevertheless, since NIrD system was solely dependent on the functional production of NS3/4A protease, this reporter is only useful for detecting early events of HCV life cycle.

In summary, we developed a cell-based dual-reporter system that demonstrates a superior ability to monitor an HCV infection in real-time. In addition to the outstanding signal/noise ratio, the NIrD system provides on-off switching signals upon HCV infection, which makes it an ideal system for the high-throughput study of HCV infections either through FACS or suicidal selection. In addition, the two reporters in the NIrD system could be substituted for other reporter types, such as luciferase[38] or SEAP[39,42], depending on specific needs. Importantly, the NIrD system is well-suited for the study of viral transmission processes, a difficult task for the majority of other reporter types[28,36,37]. Although the NIrD system is unlikely applicable for monitoring primary viruses (Supplementary Fig. 8) because these clinical strains lack the replication capability in cell culture condition, it has shown unique advantages in studies of both HCV cell-free entry and cell-to-cell transmission. In combination with current gene editing tools[31,45–47], NIrD is a robust and powerful system for the study of complex host responses to HCV, particularly in a high-throughput fashion based on a CRISPR/Cas9 library screening. A more thorough investigation of the NIrD system that uses a library that targets all protein-encoding genes is highly desirable and is highly likely to reveal comprehensive information regarding host mechanisms in response to HCV infections.
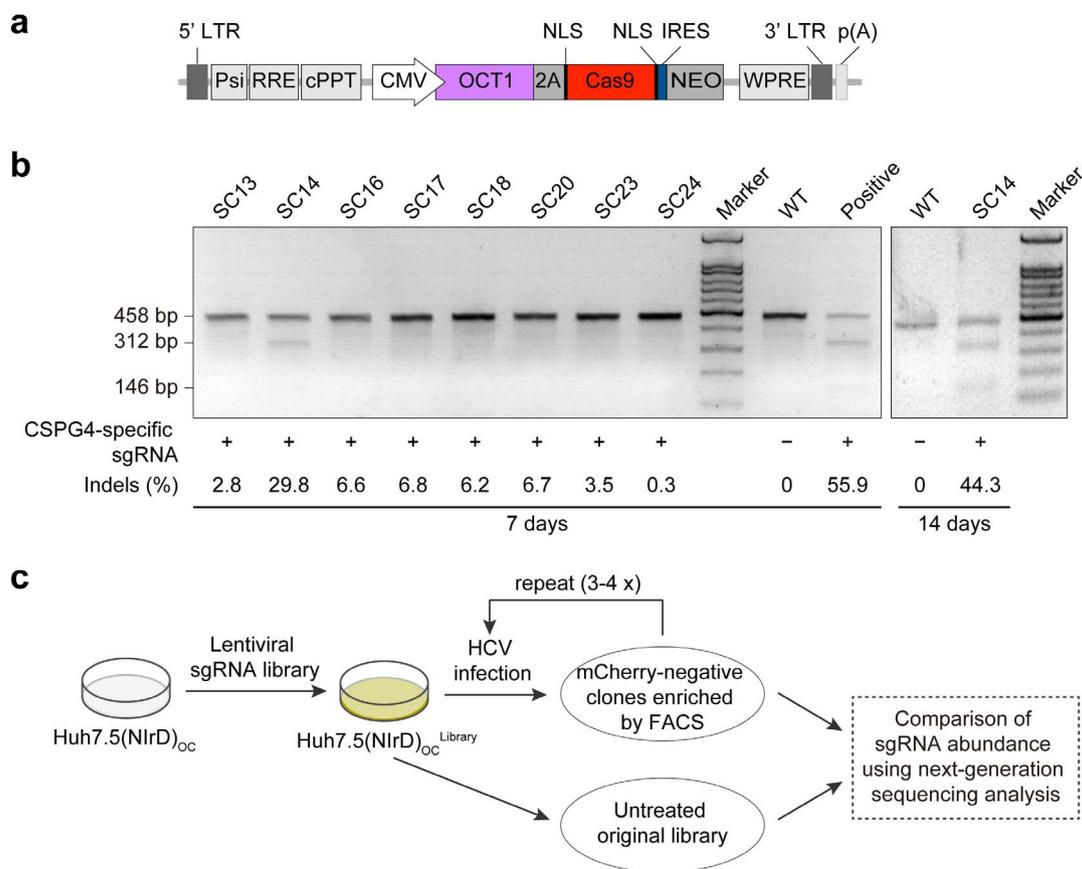
Methods

Figure 3 | Schematic of the CRISPR library construction and HCV screening. (a) The structure of the lentiviral plasmid expressing OCT1 and Cas9. (b) Indels induced by the lentivirus-delivered sgRNA (5-TTGGCCAGACTTGCATCCG-3) targeting the *CSPG4* gene in the indicated cells were assayed by T7E1 digestion. Genomic DNA from HeLa$_{OC}$-SC[31] was used as a positive control, and the wild type (WT) Huh7.5(NIrD) was used as a negative control. (c) Schematic of the sgRNA library screening. sgRNAs were delivered into Huh7.5(NIrD)$_{OC}$-SC cells by lentiviral infection with a MOI of 0.1. Three replicates of the libraries were challenged with 3–4 rounds of HCVcc, followed by FACS sorting to enrich the mCherry-negative clones. A comparison of the abundance of sgRNAs between the treated and untreated populations through high-throughput sequencing analysis was conducted following the same procedure as previously reported[31].

Plasmid construction. The pLenti-NIrD plasmid was constructed through standard cloning methods, and the sequences of the primers and plasmids are available upon request. All modules were inserted into a lentiviral vector, pLentiCMVMCSSVBsd. The CMV promoter was replaced with the tight-TRE promoter (from pEN_TTmcs), and DNA fragments coding delta-TK (a modified version of HSV-TK), 2A (2A of the Thosea asigna virus) and mCherry were concatenated sequentially. rtTA-MAVS(C)-IRES was inserted between the SV40 promoter and the Blasticidin marker gene. rtTA was cloned from pSLIK-Neo-TGmiR-Luc, and MAVS(C) (residues 462–540 of MAVS) was PCR-amplified from HeLa cDNA. The IRES sequence was obtained from pcDNA6HASIRESPuro. The TALENs plasmids were constructed using the ULtiMATE protocol[33] developed in our lab. pLenti-OC-IRES-Neo was modified from the pLenti-OC-IRES-BSD plasmid[31]. CLDN1, CD81 and OCLN expression plasmids were constructed on pLentiCMVPuroDEST, pMSCVpuro and pLentiCMVMCSSVNeo, respectively.

Construction of the CRISPR/Cas9 sgRNA library. We constructed a focused CRISPR/Cas9 library based on a previously reported library[31] with the addition of 52 sgRNAs that targeted 9 genes and included 15 non-targeting sgRNAs as negative controls. This library consisted of 918 sgRNAs, targeting a total of 296 genes.

CRISPR/Cas9 sgRNA library screening and candidate sgRNA identification. In total, 4×10^6 library cells were seeded per 150 mm petri dish as one replicate, and a total of three replicates were used for screening. After 24 h, library cells were infected by HCVcc[48] (26,666 TCID50/ml) in the presence of Dox (2 μg/ml). The original Huh(NIrD)$_{OC}$-SC14 cells were also challenged with HCV as controls. The medium was changed to fresh DMEM 24 h post infection, and the cells were harvested in another 48 h for FACS analysis to collect those cells that were mCherry negative. Cells were cultured with 2 μg/ml Dox throughout the treatment. This process was repeated 3–4 times until greater than 99% of the library cells showed no red fluorescence upon HCVcc inoculation. The high-throughput sequencing analysis and identification of the sgRNAs from the 3 replicates and the untreated libraries was conducted following the same protocol as previously reported[31].

Statistical analysis. The computational program[32] developed in the lab of Dr. Xiaole Liu at Harvard was used to perform the statistical analysis. We built a negative binomial model to calculate FDR values, and positively selected genes were those with FDR values less than 0.05.

FACS analysis. Prior to FACS analysis, Huh7.5(NIrD)$_{OC}$ cells were infected with various concentrations of HCVcc with a fixed Dox level of 2 μg/ml for 72 h. Then, cells were washed by PBS three times and harvested using 0.005% trypsin. Harvested cells were washed twice with PBS and once with FACS buffer (PBS/3% FBS) prior to analysis using a BD FACSAria™ III flow cytometer. FACS data analysis was performed using BD FACSDiva™ software.

Cell-to-cell transmission of HCV. Wild-type Huh7.5 cells were infected by EGFP-labelled HCVcc[28] for 24 h and then co-cultured with Huh7.5(NIrD) cells with a different background (WT, $CLDN1^{-/-}$, $CLDN1^{-/-}$/CLDN, $OCLN^{-/-}$, $OCLN^{-/-}$/OCLN, $CD81^{-/-}$ or $CD81^{-/-}$/CD81). After 72 h of co-culturing, the cells were washed with PBS 2 times prior to fluorescence microscopy analysis.

Immunofluorescence microscopy. Huh7.5(NIrD) cells (2×10^5 per well) were grown in 6-well plate, with a coverslip in each well. Cells were infected by HCVcc[48] with low MOI in the presence of Dox (2 μg/ml) for 72 h before fixed with PBS containing 4% methanol overnight at 4°C. Mouse anti-core mAb (1:100, Abcam #ab2740) and Alexa Fluor 488 goat anti-mouse IgG (H + L) antibody (1:1000, Life Technologies A-11029) were sequentially incubated with the sample for 1 h at 37°C, followed by PBS washing. Images were taken by DeltaVision Elite (Applied Precision, Issaquah, WA). Detailed protocol is the same as previously described[49].

Preparation and titration of HCVcc. Seed Huh7.5 cells (4×10^6/150-mm dish) one day before HCVcc infection. The virus was harvested from the supernatant through centrifugation after 4 days of initial viral infection. The virus was stocked at −40°C. HCVcc titration was performed by seeding Huh7.5(NIrD) cells (1×10^4 cells/well) in 96-well plates. Virus stock was serially diluted (10×) in DMEM medium prior to infection (100 μl of diluted virus/well, and typically 6 wells per dilution). The titre was
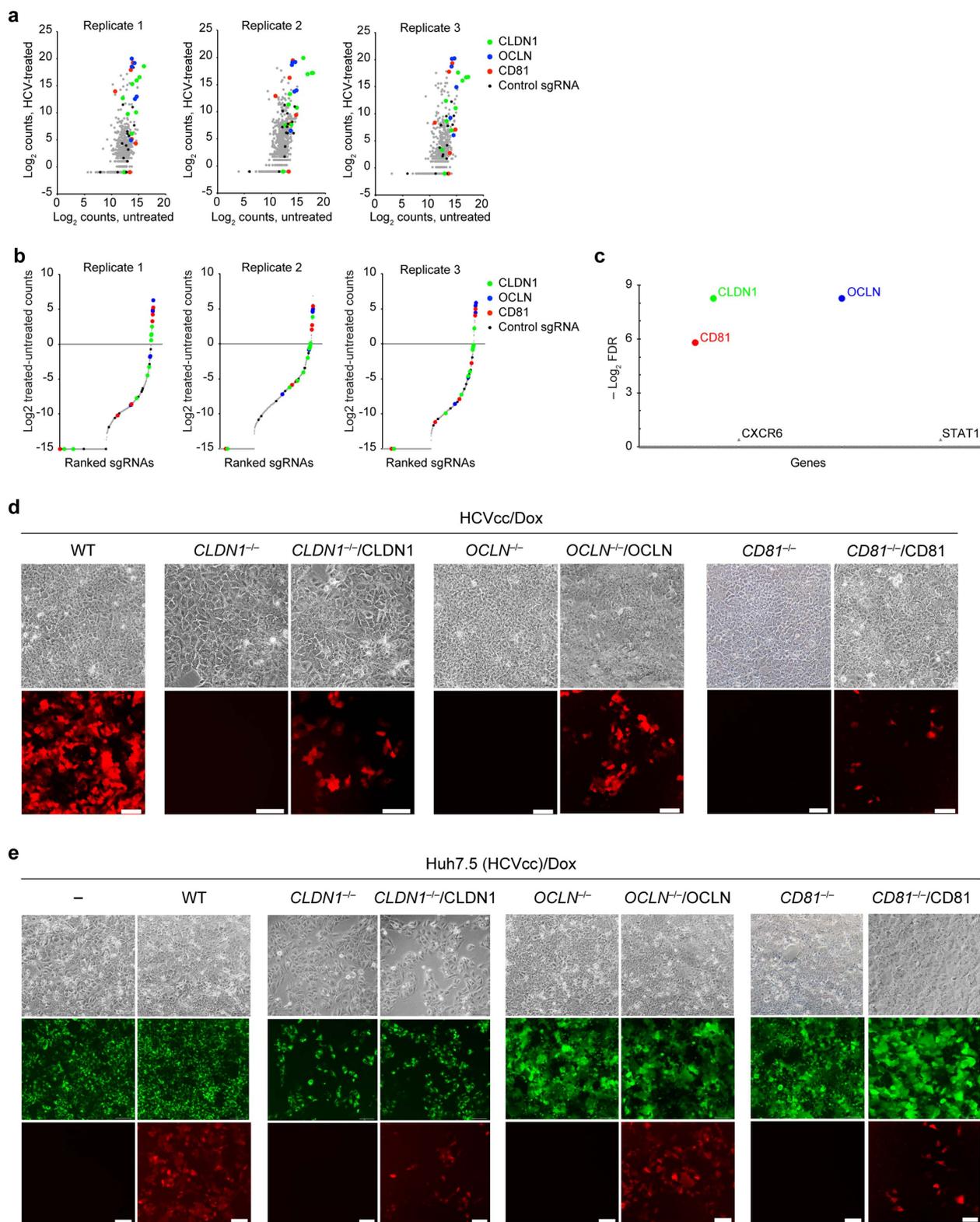
Figure 4 | Screen of host genes essential for an HCV infection. (a) Primary HCVcc screening data. The count of every sgRNA is the number of reads that match the sgRNA target sequence. (b) sgRNA ranking was based on the fold change of normalised counts of every sgRNA in the HCV treated and untreated populations. (c) The FDR (false discovery rate) of every gene in the library was calculated by MAGeCK[32] based on the counts and kinds of sgRNAs in the three replicates. (d) Effects of the gene knockout of CLND1, OCLN and CD81 on cell-free entry of HCVcc. All cells indicated carry the NIrD system. Light and fluorescence images were taken 72 h post-HCVcc infection in the presence of Dox (2 μg/ml). Scale bar, 100 μm. (e) Effects of the gene knockout of CLND1, OCLN and CD81 on cell-to-cell transmission of HCVcc. Huh7.5(NIrD) cells with the indicated background (WT, *CLDN1⁻/⁻*, *CLDN1⁻/⁻*/CLDN1, *OCLN⁻/⁻*, *OCLN⁻/⁻*/OCLN, *CD81⁻/⁻* or *CD81⁻/⁻*/CD81) were co-cultured with HCVcc pre-infected (24 h prior) Huh7.5 cells. HCVcc carries the EGFP gene in its genome[28], resulting in a punctuated green fluorescence pattern in the cells. *OCLN⁻/⁻* and *CD81⁻/⁻* knockout cells expressed diffused green fluorescence because they were derived from cells expressing EGFP. The light and fluorescence (green and red) images were taken 72 h following the co-culturing of the cells. Scale bar, 100 μm.

calculated using Reed-Muench method[50,51]. MOI was calculated according to the number of particles of HCVcc (TCID50) divided by number of seeded cells.

1. Choo, Q. L. *et al.* Isolation of a cDNA clone derived from a blood-borne non-A, non-B viral hepatitis genome. *Science* **244**, 359–362 (1989).
2. Andreoni, M. *et al.* HIV-HCV co-infection: epidemiology, pathogenesis and therapeutic implications. *Eur Rev Med Pharmacol Sci* **16**, 1473–1483 (2012).
3. Moradpour, D., Penin, F. & Rice, C. M. Replication of hepatitis C virus. *Nat Rev Microbiol* **5**, 453–463 (2007).
4. Pileri, P. *et al.* Binding of hepatitis C virus to CD81. *Science* **282**, 938–941 (1998).
5. Scarselli, E. *et al.* The human scavenger receptor class B type I is a novel candidate receptor for the hepatitis C virus. *EMBO J* **21**, 5017–5025 (2002).
6. Evans, M. J. *et al.* Claudin-1 is a hepatitis C virus co-receptor required for a late step in entry. *Nature* **446**, 801–805 (2007).
7. Ploss, A. *et al.* Human occludin is a hepatitis C virus entry factor required for infection of mouse cells. *Nature* **457**, 882–886 (2009).
8. Lupberger, J. *et al.* EGFR and EphA2 are host factors for hepatitis C virus entry and possible targets for antiviral therapy. *Nature Medicine* **17**, 589–595 (2011).
9. Sainz, B., Jr. *et al.* Identification of the Niemann-Pick C1-like 1 cholesterol absorption receptor as a new hepatitis C virus entry factor. *Nat Med* **18**, 281–285 (2012).
10. Witteveldt, J. *et al.* CD81 is dispensable for hepatitis C virus cell-to-cell transmission in hepatoma cells. *J Gen Virol* **90**, 48–58 (2009).
11. Brimacombe, C. L. *et al.* Neutralizing antibody-resistant hepatitis C virus cell-to-cell transmission. *J Virol* **85**, 596–605 (2011).
12. Fofana, I. *et al.* A novel monoclonal anti-CD81 antibody produced by genetic immunization efficiently inhibits Hepatitis C virus cell-cell transmission. *PLoS One* **8**, e64221 (2013).
13. Catanese, M. T. *et al.* Different requirements for scavenger receptor class B type I in hepatitis C virus cell-free versus cell-to-cell transmission. *J Virol* **87**, 8282–8293 (2013).
14. Lindenbach, B. D. & Rice, C. M. The ins and outs of hepatitis C virus entry and assembly. *Nat Rev Microbiol* **11**, 688–700 (2013).
15. Lee, J. C., Yu, M. C., Lien, T. W., Chang, C. F. & Hsu, J. T. High-throughput cell-based screening for hepatitis C virus NS3/4A protease inhibitors. *Assay Drug Dev Technol* **3**, 385–392 (2005).
16. Tai, A. W. *et al.* A functional genomic screen identifies cellular cofactors of hepatitis C virus replication. *Cell Host Microbe* **5**, 298–307 (2009).
17. Tanaka, Y. *et al.* Establishment of an indicator cell system for hepatitis C virus. *Microbiol Immunol* **54**, 206–220 (2010).
18. Jones, C. T. *et al.* Real-time imaging of hepatitis C virus infection using a fluorescent cell-based reporter system. *Nat Biotechnol* **28**, 167–171 (2010).
19. Hsu, E. C. *et al.* Modified apoptotic molecule (BID) reduces hepatitis C virus infection in mice with chimeric human livers. *Nature Biotechnol* **21**, 519–525 (2003).
20. Lei, Y. *et al.* MAVS-mediated apoptosis and its inhibition by viral proteins. *PLoS ONE* **4**, e5466 (2009).
21. Chockalingam, K., Simeon, R. L., Rice, C. M. & Chen, Z. A cell protection screen reveals potent inhibitors of multiple stages of the hepatitis C virus life cycle. *Proc Natl Acad Sci U S A* **107**, 3764–3769 (2010).
22. Su, A. I. *et al.* Genomic analysis of the host response to hepatitis C virus infection. *Proc Natl Acad Sci U S A* **99**, 15669–15674 (2002).
23. Markusic, D., Oude-Elferink, R., Das, A. T., Berkhout, B. & Seppen, J. Comparison of single regulated lentiviral vectors with rtTA expression driven by an autoregulatory loop or a constitutive promoter. *Nucleic Acids Res* **33**, e63 (2005).
24. Das, A. T. *et al.* Viral evolution as a tool to improve the tetracycline-regulated gene expression system. *J Biol Chem* **279**, 18776–18782 (2004).
25. Meylan, E. *et al.* Cardif is an adaptor protein in the RIG-I antiviral pathway and is targeted by hepatitis C virus. *Nature* **437**, 1167–1172 (2005).
26. Shin, K. J. *et al.* A single lentiviral vector platform for microRNA-based conditional RNA interference and coordinated transgene expression. *Proc Natl Acad Sci U S A* **103**, 13759–13764 (2006).
27. Salomon, B. *et al.* A truncated herpes simplex virus thymidine kinase phosphorylates thymidine and nucleoside analogs and does not cause sterility in transgenic mice. *Mol Cell Biol* **15**, 5322–5328 (1995).
28. Han, Q. *et al.* Compensatory mutations in NS3 and NS5A proteins enhance the virus production capability of hepatitis C reporter virus. *Virus Res* **145**, 63–73 (2009).
29. Wakita, T. *et al.* Production of infectious hepatitis C virus in tissue culture from a cloned viral genome. *Nat Med* **11**, 791–796 (2005).
30. Matthews, S. J. & Lancaster, J. W. Telaprevir: a hepatitis C NS3/4A protease inhibitor. *Clin Ther* **34**, 1857–1882 (2012).
31. Zhou, Y. *et al.* High-throughput screening of a CRISPR/Cas9 library for functional genomics in human cells. *Nature* **509**, 487–491 (2014).
32. Li, W. *et al.* MAGeCK enables robust identification of essential genes from genome-scale CRISPR/Cas9 knockout screens. *Genome Biology* **15**, 554, doi:10.1186/s13059-014-0554-4 (2014).
33. Yang, J. *et al.* ULtiMATE system for rapid assembly of customized TAL effectors. *PLoS One* **8**, e75649 (2013).
34. Zeisel, M. B., Fofana, I., Fafi-Kremer, S. & Baumert, T. F. Hepatitis C virus entry into hepatocytes: Molecular mechanisms and targets for antiviral therapies. *J Hepatol* **54**, 566–576 (2011).
35. Carloni, G., Crema, A., Valli, M. B., Ponzetto, A. & Clementi, M. HCV infection by cell-to-cell transmission: choice or necessity? *Curr Mol Med* **12**, 83–95 (2012).
36. Kim, C. S., Jung, J. H., Wakita, T., Yoon, S. K. & Jang, S. K. Monitoring the antiviral effect of alpha interferon on individual cells. *J Virol* **81**, 8814–8820 (2007).
37. Schaller, T. *et al.* Analysis of hepatitis C virus superinfection exclusion by using novel fluorochrome gene-tagged viral genomes. *J Virol* **81**, 4591–4603 (2007).
38. Koutsoudakis, G. *et al.* Characterization of the early steps of hepatitis C virus infection by using luciferase reporter viruses. *J Virol* **80**, 5308–5320 (2006).
39. Pacini, L., Bartholomew, L., Vitelli, A. & Migliaccio, G. Reporter substrates for assessing the activity of the hepatitis C virus NS3-4A serine protease in living cells. *Anal Biochem* **331**, 46–59 (2004).
40. Breiman, A. *et al.* A hepatitis C virus (HCV) NS3/4A protease-dependent strategy for the identification and purification of HCV-infected cells. *J Gen Virol* **87**, 3587–3598 (2006).
41. Lei, Y. F. *et al.* Development of a cell-based assay for monitoring hepatitis C virus ns3/4a protease activity. *Acta Virol* **52**, 133–141 (2008).
42. Pan, K. L., Lee, J. C., Sung, H. W., Chang, T. Y. & Hsu, J. T. Development of NS3/4A protease-based reporter assay suitable for efficiently assessing hepatitis C virus infection. *Antimicrob Agents Chemother* **53**, 4825–4834 (2009).
43. Lee, J. C. *et al.* A cell-based reporter assay for inhibitor screening of hepatitis C virus RNA-dependent RNA polymerase. *Anal Biochem* **403**, 52–62 (2010).
44. Li, X. D., Sun, L., Seth, R. B., Pineda, G. & Chen, Z. J. Hepatitis C virus protease NS3/4A cleaves mitochondrial antiviral signaling protein off the mitochondria to evade innate immunity. *Proc Natl Acad Sci U S A* **102**, 17717–17722 (2005).
45. Miller, J. C. *et al.* A TALE nuclease architecture for efficient genome editing. *Nat Biotechnol* **29**, 143–148, doi:10.1038/nbt.1755 (2011).
46. Cong, L. *et al.* Multiplex Genome Engineering Using CRISPR/Cas Systems. *Science*, doi:10.1126/science.1231143 (2013).
47. Mali, P. *et al.* RNA-guided human genome engineering via Cas9. *Science* **339**, 823–826, doi:10.1126/science.1232033 (2013).
48. Jiang, J. & Luo, G. Cell culture-adaptive mutations promote viral protein-protein interactions and morphogenesis of infectious hepatitis C virus. *J Virol* **86**, 8987–8997 (2012).
49. Qian, L. *et al.* Bidirectional effect of Wnt signaling antagonist DKK1 on the modulation of anthrax toxin uptake. *Science China. Life sciences* **57**, 469–481 (2014).
50. Reed, L. J. & Muench, H. A simple method of estimating fifty per cent endpoints. *Am. J. Epidemiol.* **27**, 493–497 (1938).
51. Lindenbach, B. D. *et al.* Complete replication of hepatitis C virus in cell culture. *Science* **309**, 623–626 (2005).

Acknowledgments

Author contributions

W.W., Q.R. and C.L. conceived the methodology and designed the experiments. Q.R., C.L. and C.C. performed the experiments. W.W., Q.R., C.L., P.Y. and C.C. analysed the data. L.Z. and G.L. provided the reagents and the facility. W.W., Q.R. and C.L. wrote the manuscript with the assistance of the other authors.

Additional information

Supplementary Information

A Dual-Reporter System for Real-Time Monitoring and High-throughput CRISPR/Cas9 Library Screening of the Hepatitis C Virus

Qingpeng Ren, Chan Li, Pengfei Yuan, Changzu Cai, Linqi Zhang, Guangxiang George Luo and Wensheng Wei

Biodynamic Optical Imaging Center (BIOPIC), State Key Laboratory of Protein and Plant Gene Research, School of Life Sciences, Peking University, Beijing 100871, China

*Correspondence should be addressed to W.W. (wswei@pku.edu.cn).
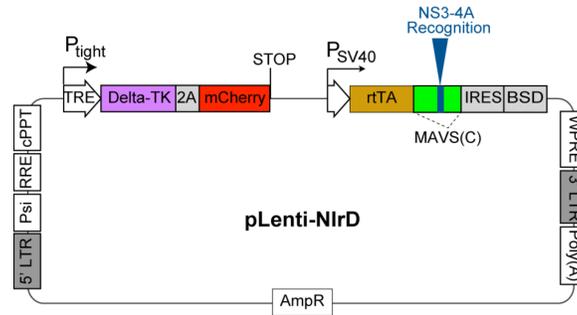
Supplementary Figure 1. Design of the NlrD construct. This reporter construct was composed of two cassettes in a pLentiCMVMCSSVBsd backbone. One cassette contains DNA sequences encoding 2A-linked delta-TK and mCherry under the control of the tight-TRE promoter (P_{tight}). The second cassette consists of the SV40 promoter-driven sequences encoding the rtTA-MAVS(C) fusion protein and Blasticidin (BSD), in which the rtTA were fused with MAVS C-terminal residues (462-540) that contain the NS3-4A recognition site (^{503}EREVPCH^{509}), and the BSD-coding region followed IRES.
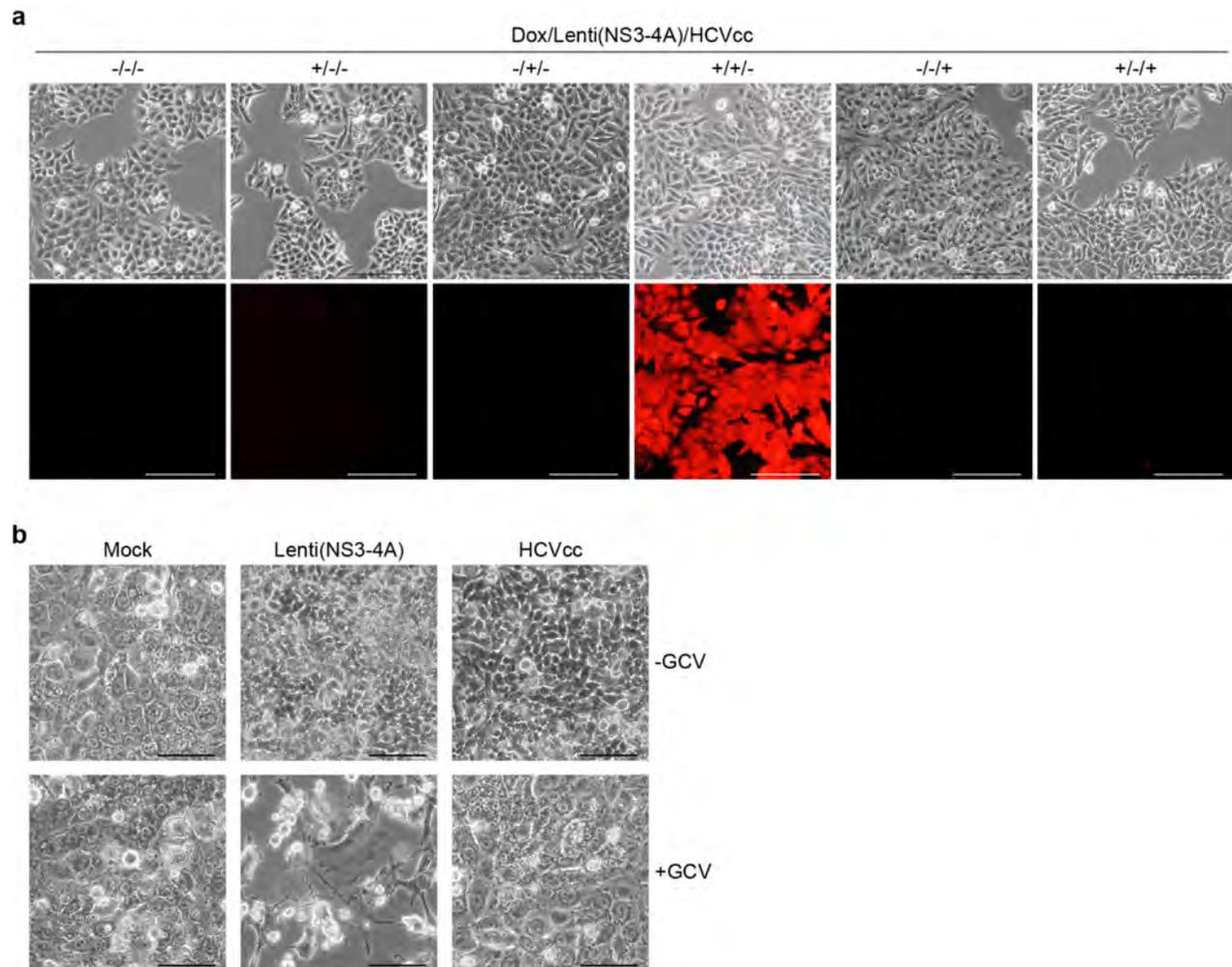
Supplementary Figure 2. The NlrD system in HeLa cells in response to NS3-4A-expressing lentivirus or HCVcc. (**a**) mCherry signal of the NlrD system in response to a viral infection. Both the light (top) and the fluorescent (bottom) images were taken 72 h post-infection with different combinations of Lenti(NS3-4A), HCVcc and Dox (2 μg/ml). Scale bar, 200 μm. (**b**) Death signal of the NlrD system in response to lentivirally delivered NS3-4A in the presence of Dox (2 μg/ml). The light images of the cells were taken 120 h post-infection in the absence (top) or presence (bottom) of GCV (2 μg/ml). Scale bar, 200 μm.
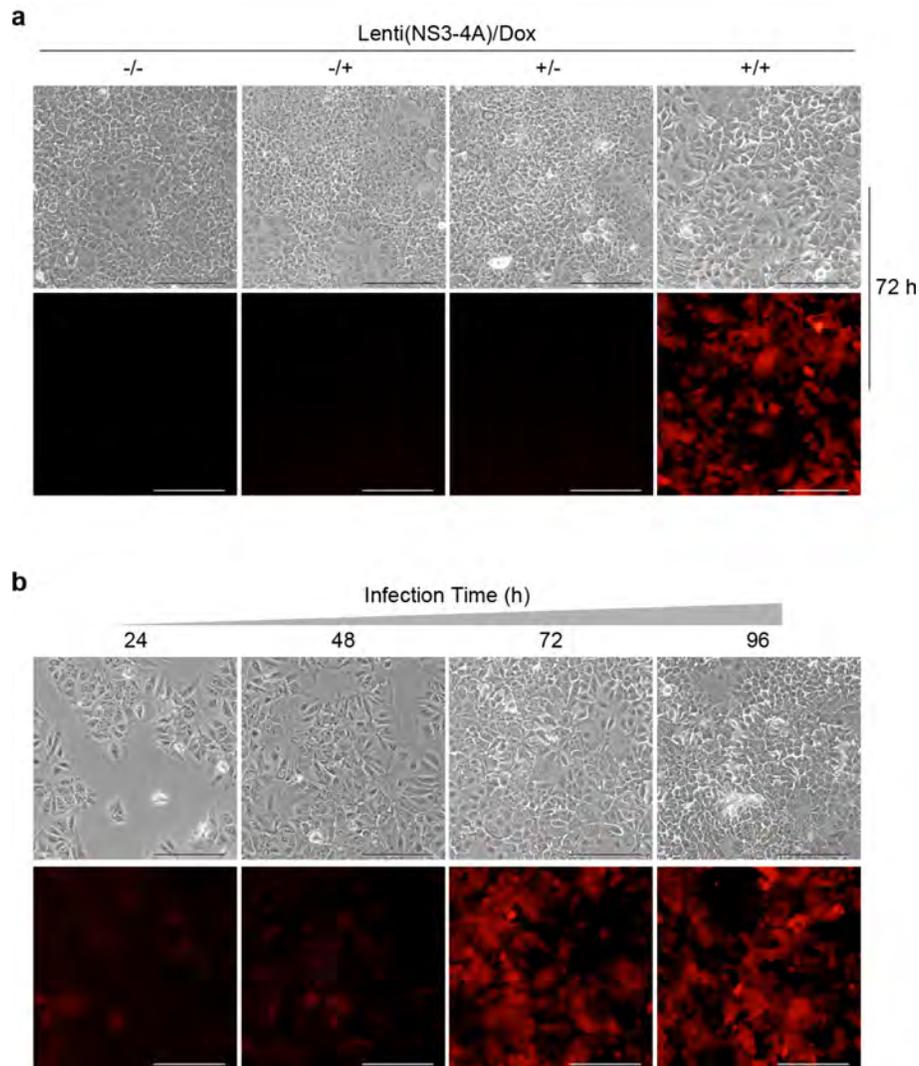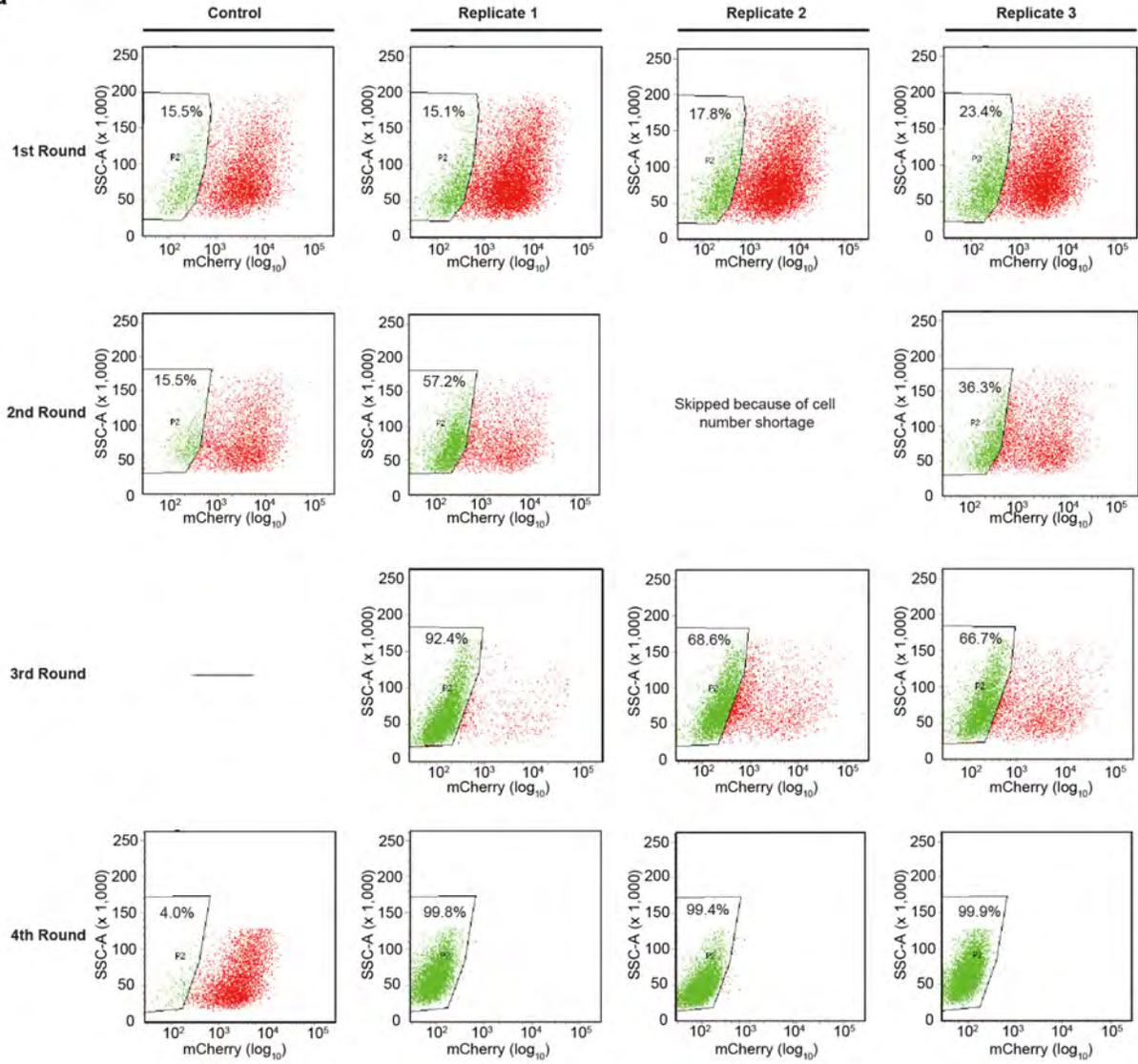
Supplementary Figure 3. The mCherry signal of the NIrD system in Huh7.5 cells in response to NS3-4A-expressing lentivirus. (**a**) Huh7.5(NIrD) cells were infected with the virus for 72 h. The virus-transduced (+) or -untransduced (−) cells in the presence (+) or absence (−) of Dox (2 μg/ml) were visualised by microscopy. Scale bar, 200 μm. (**b**) Time-lapse live-cell imaging of Huh7.5(NIrD) after NS3-4A-expressing lentiviral infection. Scale bar, 200 μm.
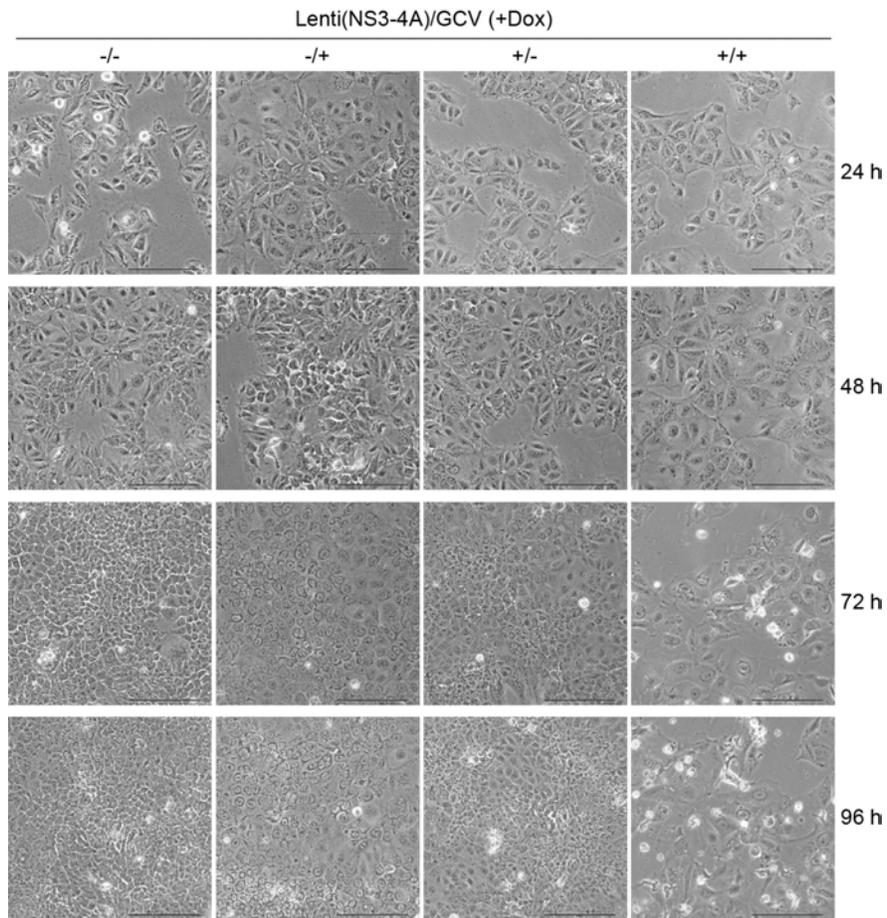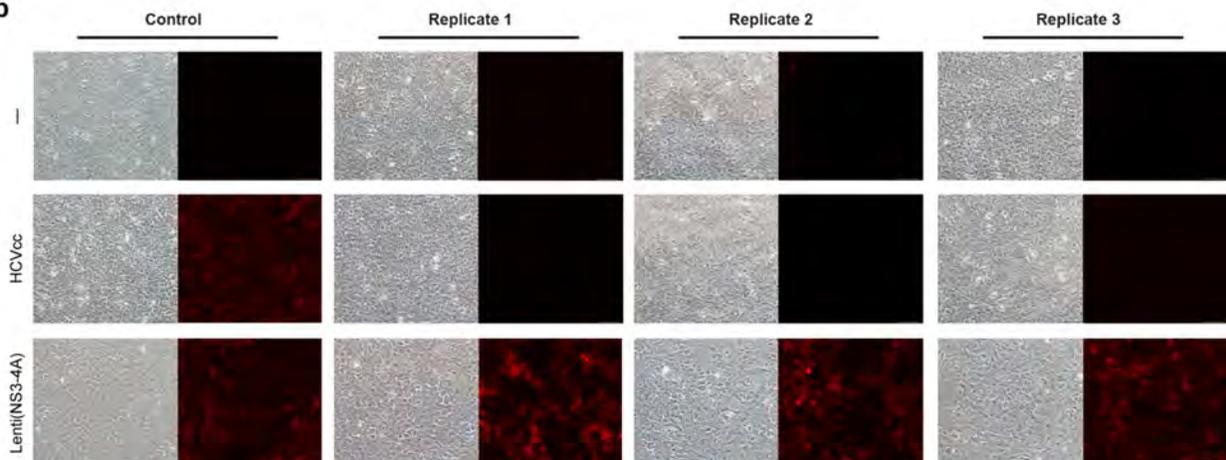
Supplementary Figure 4. Death signal of the NIrD system in Huh7.5 cells in response to NS3-4A-expressing lentivirus. Huh7.5(NIrD) cells were infected with (+) or without (−) the virus in the presence (+) or absence (−) of GCV (2 µg/ml). Dox (2 µg/ml) was supplied in all conditions. The light microscopy images were taken every 24 h, starting at 24 h post-infection. Scale bar, 200 µm.
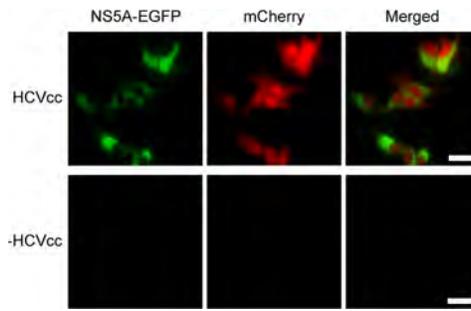
Supplementary Figure 5. Fluorescence microscopy of EGFP-conjugated NS5A and mCherry signal upon HCVcc infection (72 h) in Huh7.5(NIrD) cells. Scale bar, 30 μm.

a

	Control	Replicate 1	Replicate 2	Replicate 3

1st Round

15.5% 15.1% 17.8% 23.4%

2nd Round

15.5% 57.2% Skipped because of cell number shortage 36.3%

3rd Round

92.4% 68.6% 66.7%

4th Round

4.0% 99.8% 99.4% 99.9%

b

	Control	Replicate 1	Replicate 2	Replicate 3
–				
HCVcc				
Lenti(NS3-4A)				

Supplementary Figure 6. mCherry signals in Huh7.5(NIrD) cells during the library screening.

(**a**) FACS analysis of control Huh7.5(NIrD) cells and three replicates of the CRISPR libraries throughout 3-4 rounds of HCVcc infections. In each round, 4×10^6 cells were infected by HCVcc (26,666 TCID50/ml) plus Dox (2 µg/ml), followed by FACS at 72 h post-viral infection. The original Huh7.5(NIrD) was used as the control for this and the remaining figures. (**b**) mCherry-negative cells in three library replicates following the 4th round of FACS were assayed through fluorescence microscopy on their internal NIrD system in response to NS3-4A-expressing lentivirus or HCVcc. Scale bar, 100 µm.

a

```
TGTCCTGCGTGTCGCAGAGCACCGGG----------------------------CAGATCCAGTGCAAAGTCTTTGA    Wild-type
        TALENᴸ                                                    TALENᴿ
TGTCCTGCGTGTCGCAGAGCACCGGGATGCGCGTGGGTGAAGCCGTGACCCACCGGGCAGATCCAGTGCAAAGTCTTTGA    CLDN1⁻ᐟ⁻ (+31)
```

b

```
AATCATTATGCACCAAGCAATGAC---AT-A-TATG-----------GTGGAGAGATGCATGTTC    Wild-type
               sgRNA
AATCATTATGCACCAAGCAATGACCGAATCATTATGCACCAAGCAATGGTGGAGAGATGCATGTTC    OCLN⁻ᐟ⁻ (+17)
```

c

```
AGGCGTGATCCTGGGTGTGGCCCTGTGGCTCCGCCATG    Wild-type
        sgRNA
AGGCGTGATCCTGGGTGTGGC--------TCCGCCATG    CD81⁻ᐟ⁻ (Δ8)
```

Supplementary Figure 7. Gene knockouts of CLDN1, OCLN and CD81 in Huh7.5(NlrD). (**a**) Partial sequences of the *CLDN1* gene in a genome containing TALENs binding regions (underlined) and the mutated alleles from the TALENS clone. The tall letter indicates an insertion and the dashes indicate a deletion in this and other figures. The primers used to amplify the TALENs targeting region for sequencing analysis are 5'-GTTGCCCACCTGCAAACTCTCC-3' and 5'-TGTCACCCAGGGAGTTAGAGGC-3'. (**b-c**) DNA sequencing analysis of mutated alleles in OCLN (**b**) and CD81 (**c**) loci. Partial coding sequences of the targeted genes in the genome containing the CRISPR/Cas9 sgRNA^OCLN or sgRNA^CD81 binding regions (underlined) and the sequence analysis of the mutated alleles are shown. The shaded nucleotides represent the PAM sequences that guide Cas9 for DNA recognition and cleavage. The primers used to amplify the sgRNA-targeting regions for sequencing analysis are 5'- ACCCCCAAACAGAGATAACCC-3' + 5'-GCCTACACTACCTCCTAAAAGGG-3' (for OCLN), and 5'- AGGGCCAGGCTCCAAGTAG-3' + 5'- ACACGCCATGCCCGACT-3' (for CD81).
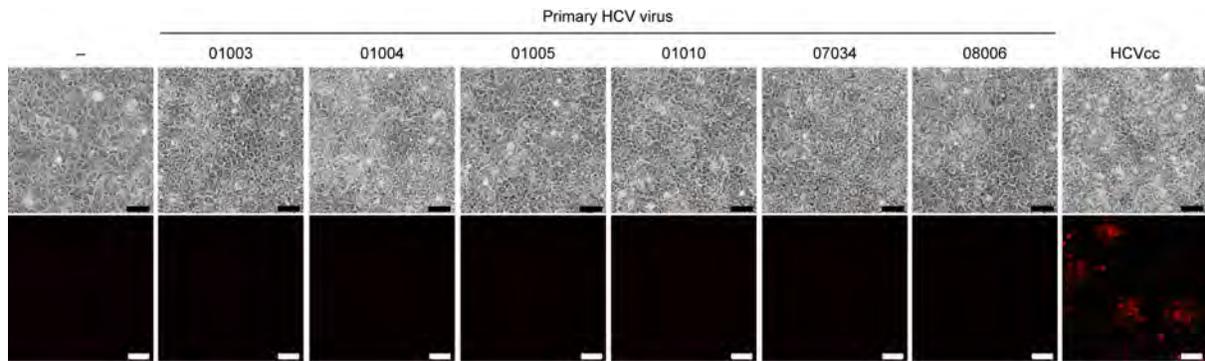
Supplementary Figure 8. The mCherry signal of the NlrD system in Huh7.5 cells in response to HCV infection. Total of 6 serum samples from different HCV patients were used at high MOI (Titer of viral samples was obtained by Abbott Realtime™ Test Assays), 01003 (genotype 2), 01004 (genotype 1b), 01005 (genotype 1b), 01010 (genotype 2), 07034 (genotype 3a) and 08006 (genotype 6a/6b). Cells were infected by virus in the presence of Dox (2 μg/ml) for 72 h before observation under microscope. Scale bar, 100 μm.